

MIT Open Access Articles

Artificial Anti-Tumor Opsonizing Proteins with Fibronectin Scaffolds Engineered for Specificity to each of the Murine Fc γ R Types

The MIT Faculty has made this article openly available. **Please share** how this access benefits you. Your story matters.

As Published: 10.1016/J.JMB.2018.04.021

Publisher: Elsevier BV

Persistent URL: <https://hdl.handle.net/1721.1/134976>

Version: Author's final manuscript: final author's manuscript post peer review, without publisher's formatting or copy editing

Terms of use: Creative Commons Attribution-NonCommercial-NoDerivs License





Published in final edited form as:

J Mol Biol. 2018 June 08; 430(12): 1786–1798. doi:10.1016/j.jmb.2018.04.021.

Artificial Anti-tumor Opsonizing Proteins with Fibronectin Scaffolds Engineered for Specificity to Each of the Murine Fc γ R Types

Tiffany F. Chen^{1,3}, Kevin K. Li^{1,3}, Eric F. Zhu^{2,3}, Cary F. Opel^{2,3}, Monique J. Kauke^{2,3}, Heeyoon Kim³, Eta Atolia³, and K. Dane Wittrup^{1,2,3}

¹Department of Biological Engineering, Massachusetts Institute of Technology, 77 Massachusetts Ave., Cambridge, MA 02139, United States

²Department of Chemical Engineering, Massachusetts Institute of Technology, 77 Massachusetts Ave., Cambridge, MA 02139, United States

³Koch Institute for Integrative Cancer Research, Massachusetts Institute of Technology, 77 Massachusetts Ave., Cambridge, MA 02139, United States

Abstract

We have engineered a panel of novel Fn3 scaffold-based proteins that bind with high specificity and affinity to each of the individual mouse Fc γ receptors (mFc γ R). These binders were expressed as fusions to anti-tumor antigen single chain antibodies and mouse serum albumin, creating opsonizing agents that invoke only a single mFc γ R response rather than the broader activity of natural Fc isotypes, as well as all previously reported Fc mutants. This panel isolated the capability of each of the four mFc γ Rs to contribute to macrophage phagocytosis of opsonized tumor cells, and *in vivo* tumor growth control with these monospecific opsonizing fusion proteins. All activating receptors (mFc γ RI, mFc γ RIII, and mFc γ RIV) were capable of driving specific tumor cell phagocytosis to an equivalent extent, while mFc γ RII, the inhibitory receptor, did not drive phagocytosis. Monospecific opsonizing fusion proteins that bound mFc γ RI alone controlled tumor growth to an extent similar to the most active IgG2a murine isotype. As expected, binding to the inhibitory mFc γ RII did not delay tumor growth, but unexpectedly mFc γ RIII also failed to control tumor growth. mFc γ RIV exhibited detectable but lesser tumor-growth control leading to less overall survival compared to mFc γ RI. Interestingly, *in vivo* macrophage depletion demonstrates their importance in tumor control with mFc γ RIV engagement, but not with mFc γ RI.

Correspondence Addressed to: K. Dane Wittrup, C.P. Dubbs Professor, Chemical Engineering & Biological Engineering, Assoc. Dir., Koch Institute for Integrative Cancer Research, Massachusetts Institute of Technology, Bldg 76-261D, 500 Main Street, Cambridge, MA 02139, PH 617-253-4578, wittrup@mit.edu.

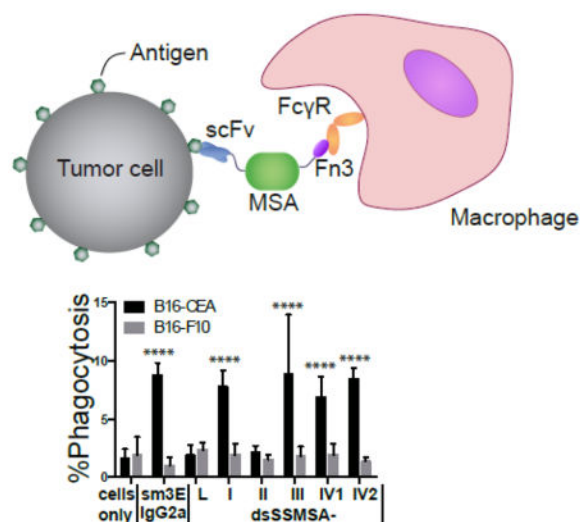
Author Contributions: T.F.C. and K.D.W. designed research and wrote the paper. T.F.C., K.K.L., E.F.Z., C.F.O. performed research. T.F.C., E.F.Z., C.F.O., and K.D.W. analyzed data. M.J.K., H.K., and E.A. provided technical assistance.

Conflict of Interest: T.F.C. is currently an employee of Rubius Therapeutics. E.F.Z. is currently an employee of Cygnal Therapeutics. C.F.O. is currently an employee of Gilead Sciences. The other authors declare no potential conflicts of interest.

Publisher's Disclaimer: This is a PDF file of an unedited manuscript that has been accepted for publication. As a service to our customers we are providing this early version of the manuscript. The manuscript will undergo copyediting, typesetting, and review of the resulting proof before it is published in its final citable form. Please note that during the production process errors may be discovered which could affect the content, and all legal disclaimers that apply to the journal pertain.

This panel of monospecific mFc γ R binding proteins provides a toolkit for isolating the functional effects of each mFc γ R in the context of an intact immune system.

Graphical Abstract



Keywords

Fc gamma receptor; cancer; yeast display; alternative scaffold; macrophage

Introduction

Monoclonal antibodies (mAb) operate through various mechanisms for cancer therapy: blocking receptor signaling; delivery of toxic chemotherapy through antibody drug conjugates; or triggering the immune system (i.e. antibody-dependent cellular cytotoxicity (ADCC)) [1–4]. Fc γ receptors (Fc γ Rs) modulate immune cell interaction with IgG Fc's. It has been proposed that the balance between activating and inhibiting Fc γ R signaling (A/I ratio) determines the effectiveness of effector functions, prompting extensive protein engineering and glycoengineering efforts to shift the balance of Fc binding affinity towards the activating receptors and away from the inhibitory receptor [5–13].

The distribution of Fc γ Rs is approximately conserved between humans and mice, enabling mice as useful animal models for therapeutics development [14]. Humans express the activating receptors: Fc γ RI, Fc γ RIIA, Fc γ RIIC, and Fc γ RIIIA, the inhibitory receptor Fc γ RIIB, and GPI-linked Fc γ RIIIB. Mice express Fc γ RI (CD64), Fc γ RIII (CD16), and Fc γ RIV (CD16-2) as activating receptors and Fc γ RIIB (CD32) as an inhibitory receptor. Fc γ Rs on immune cells bind to antibody immune complexes and trigger signaling pathways of innate effector cells leading to the release of reactive oxidative species, phagocytosis, and other cytotoxic effector functions.

In mAb cancer therapeutics, activating Fc γ Rs have been shown to play a key role in the elimination of tumor cells [15]. A landmark example is the α -CD20 mAb, rituximab, and its

mechanism of action through Fc γ RIIIa engagement [7]. The role of different Fc γ Rs has been studied through different knockout (KO) mice and antibody isotypes. Nimmerjahn and Ravetch showed that *in vivo* the IgG2a isotype was most effective in mediating effector functions with the B16F10 lung metastasis mouse model treated with the anti-TRP1 antibody TA99. Different Fc γ R KO mice injected with B16F10 melanoma cells and treated with the TA99 IgG2a antibody revealed that Fc γ RIV played the major role in tumor clearance [5]. Subsequent work has revealed overlapping roles for Fc γ RI and Fc γ RIV in tumor cytotoxicity [16,17].

Close homology amongst the Fc γ Rs in any given species makes it virtually impossible to engineer the natural Fc/Fc γ R interface for absolute specificity to only one Fc γ R. Both the amino acid sequence and the particular glycoforms attached to asparagine 297 of the Fc impact Fc γ R binding affinity to IgGs [14]. Past studies have shown the importance of different fucosylation and sialylation of IgGs on ADCC [6,18–20]. Selection of amino acid mutants has also been performed through computational predictions and alanine scanning [9,21].

Bispecific antibodies linking tumor antigens and human CD16 (Fc γ RIIIa) have proven successful in preclinical models in directing NK activity against tumor models [22,23]. Engineering alternative scaffolds to target human Fc γ RIIIa has shown promising *in vitro* and *in vivo* results [24,25]. In this study, we engineer binders based on the human tenth type III fibronectin (Fn3) scaffold [26–28] that are highly specific to each of the individual four mouse Fc γ Rs. The approach described here will be useful for studying antibody effector functions in mouse models. A mouse model with human Fc γ Rs has been developed [29] and an approach similar to ours could be used to help parse out the roles of individual human Fc γ Rs in that model system.

Results

Homology modeling of mFc γ Rs to human Fc γ Rs

The murine Fc γ Rs (mFc γ R) were homology modeled onto the equivalent human crystal structures (Fig. 1a), and the Fc binding region is outlined in red, green, and blue, representing BC loop, C'E loop, and FG loop interaction epitopes, respectively. As noted, the areas of interaction are all in the same region of the Fc γ Rs. The sequence alignment shows the similarity between the different Fc γ Rs, especially mFc γ RIIB and mFc γ RIII (Fig. 1b). At the Fc γ R-binding region, there is only one amino acid difference between mFc γ RIIB and mFc γ RIII, therefore making it especially difficult to engineer the antibody Fc to highly differentiate between the two receptors. Furthermore, the Fc γ R monomer interacts with each domain of the CH2 homodimer of IgGs in a non-symmetric fashion. Because the Fc is a homodimer, it would be difficult to completely decouple binding with different Fc γ Rs with only mutagenesis of the IgG Fc region, unless the Fc is engineered as a heterodimer [30]. An alternative approach, and the one used in this work, is to utilize different scaffolds in place of the Fc region as binders for Fc γ Rs.

Sorting Methodology for Fn3 binders to mFcγRs

In order to engineer binders with specificity to an individual mFcγR with low cross-reactivity to the other mFcγRs, we had to implement a selective sorting strategy. The Fn3 yeast surface-displayed G4 library [31] was sorted separately against each biotinylated mFcγR ectodomain with stringent depletions (Fig. 2a) against naked beads and pools of the other three mFcγR (Fig. 2b) before enrichment of binders to target mFcγRs (RI, RIIB, RIII, and RIV). After low affinity Fn3 binders were enriched with magnetic beads, sorting was performed by fluorescence-activated cell sorting (FACS). Two methods with FACS were used to isolate non-cross-reactive Fn3 binders. In one sorting method, Fn3 clones that bound to the target mFcγR were enriched before sequentially depleting clones that bound to a different mFcγR (Fig. 2c). Clones that displayed Fn3 properly but showed no cross-reactivity to the non-target mFcγR were enriched. In the other sorting method, tetramers of biotinylated mFcγR bound to streptavidin were incubated with sublibraries and sorted for binders specific to the target mFcγR (Fig. 2d). Previous literature suggested the importance of mFcγRIV in tumor clearance [5], so two different sorts were conducted targeting mFcγRIV.

Isolated Fn3 Clones Specific for Individual mFcγR

Titration of different concentrations of soluble target mFcγR ectodomain were performed on a panel of isolated Fn3 clones expressed on yeast surface display and binding was detected on flow cytometry. A single clone from each group with the highest maximum fluorescence and lowest apparent K_D was chosen for further studies. These clones were renamed I, II, III for Fn3 binders specific to mFcγRI, mFcγRIIB, and mFcγRIII, respectively (Table S1). Two different clones, renamed IV1 and IV2, were chosen from the different sorts conducted on mFcγRIV (Table S1).

Since two different Fn3s against mFcγRIV were isolated, we were interested where they bound on the receptor. The binding epitopes of the two Fn3 binders IV1 and IV2 to mFcγRIV were determined using a yeast display epitope-mapping library of mFcγRIV. Briefly, the ectodomain of mFcγRIV was cloned into the yeast display vector and subjected to a low level of mutagenesis to obtain a small library of mFcγRIV with single point mutations. Fn3 binding epitopes were determined by isolation of clones that were mutated in the mutagenesis screen that no longer showed binding to the Fn3. IV1 was mapped to domain 2 of mFcγRIV at residues Q122/K127/K128 (Fig. 3a), and IV2 was mapped to domain 1 at residues K38/R67/Q69 (Fig. 3b). Interestingly, the IV2 epitope was distinct from the actual mFcγRIV/Fc interface; consequently, it was possible to test whether precise stereospecific engagement of FcγRs were required for activation.

To demonstrate low to no cross-reactivity, titration of all mFcγR were conducted on each yeast displayed Fn3 clone (Fig. 3c). Clones I, IV1, and IV2 showed very high specificity for their respective mFcγR and no detectable binding to the other mFcγRs. Clone II appeared to be high affinity to mFcγRIIB, but had very slight binding to mFcγRIII at 1 μM concentration. Clone III was also a specific albeit weaker binder to mFcγRIII when compared to the other Fn3 clones and their respective mFcγRs, exhibiting slight cross-reactivity to mFcγRIV at 1 μM concentration. The low cross-reactivity of clones I, III, IV1,

and IV2 suggests a high A/I ratio, since binding to the inhibitory receptor is barely detectable.

Engineered scFv-MSA-Fn3 Construct

A tumor targeting fusion protein was engineered using a single chain variable fragment (scFv) at the N-terminus followed by a mouse serum albumin (MSA) and then a particular mFcγR-binding Fn3 (Fig. 4a), with the domains separated by linkers. The scFv, sm3E, was previously engineered to have high affinity to the tumor antigen carcinoembryonic antigen (CEA) with a K_D of 30pM [32]. The scFv was disulfide stabilized by introducing two cysteine residues at R44C in framework region 2 (FR2) of the heavy chain and G100C in FR4 of the light chain [33]. MSA was used in the protein fusion construct to confer several useful characteristics: 1) enhanced serum half-life [34], 2) no residual interaction with mFcγR, and 3) low immunogenicity. Serum albumin exhibits a long serum half-life through its interactions with FcRn [35], while not interacting with any of the mFcγRs [36]. A construct was made with each mFcγR binding Fn3 and a separate negative control Fn3, L7.5.1, a picomolar binder to hen-egg lysozyme [37], renamed L. Construct nomenclature was denoted “dsSSMSA-Fn3 clone”, with “ds” representing disulfide stabilized and the “SS” representing sm3E scFv.

Binding Functionality of dsSSMSA-Fn3

Binding functionality of the dsSSMSA-Fn3 constructs was determined using flow cytometry on four cell lines: the antigen positive MC38-CEA and B16-CEA cell lines along with the antigen negative cell lines MC38 and B16-F10. All constructs showed specific binding to only CEA positive cell lines and no binding to antigen negative cell lines (Fig. S1a–b). Two clonally distinct cell lines were used to confirm that this format was applicable to various model systems.

Constructs were tested to see if they could simultaneously bind CEA positive cells and fluorophore labeled streptavidin tetramers of their target biotinylated mFcγR (Fig. 4b) with flow cytometry. Normalized heat maps were used to represent flow cytometry data (Fig. S1c–d) in a simplified format. As expected, dsSSMSA-L showed no binding to any of the mFcγRs, while the remaining constructs had exquisite specificity to their respective mFcγR (Fig. 4c and d) on both MC38-CEA and B16-CEA cell lines. The amount of binding of dsSSMSA-III was slightly less than the other dsSSMSA-Fn3s, which is reflective of the original titration data. The IV1 Fn3 also had lower binding to mFcγRIV than IV2, and these results were true for both cell lines. These binding results show that the engineered dsSSMSA-Fn3 constructs can simultaneously bind CEA positive tumor cells and engage with mFcγRs, enabling specific bridging of target cells to individual mFcγRs.

Binding Kinetics

Equilibrium binding constants of each Fn3 to their respective mFcγR was determined through using a ForteBio BLitz machine (Fig. S2). All Fn3 binders range from mid to low nM K_D s with binder I having a K_D of 19.9 nM, II with a 7.5 nM K_D , III with a 44.0 nM K_D , and with binders IV1 and IV2 having similar K_D s of 29.1 and 28.9 nM, respectively (Fig. 4e). Binder I had a slower k_{on} than the other binders, but also had a slower k_{off} and therefore

was a mid-affinity binder. The mFc γ RIIB binder II, on the other hand, had relatively average k_{on} but a slower k_{off} leading to a lower K_D than the other binders. The III binder had a slightly higher K_D compared the other binders which agreed with the yeast surface titration data. The mFc γ RIV binder IV1 had a slightly slower k_{on} and k_{off} compared to IV2, therefore leading to similar K_D values.

Binding on Fc γ Rs expressing cells

To confirm that these constructs could bind to cells expressing Fc γ Rs, HEK293 cells were transiently transfected with the full mFc γ Rs along with the common γ -chain for the activating Fc γ Rs (Fig. S3a). The dsSSMSA-I, III, IV1, and IV2 constructs showed very specific binding to their target Fc γ Rs (Fig. 5a and Fig. S3b). Murine B-cells were used to confirm dsSSMSA-II binding, since they only express mFc γ RIIB. Primary mouse splenocytes were isolated and stained for the CD19+B220+ B-cell markers along with dsSSMSA-II. We gated on CD19+B220+ cells and within that population we detected a small population that bound dsSSMSA-II while not binding the control dsSSMSA-L (Fig. 5b). We confirmed that not only do our constructs specifically bind antigen positive tumor cells, but also are able to bind mFc γ R expressing cells.

Phagocytosis Assay

A phagocytosis assay was conducted to determine if these engineered constructs promoted mFc γ R-driven effector functions. Tumor cells labeled with carboxyfluorescein succinimidyl ester (CFSE) were pre-coated with the protein constructs and then incubated with peritoneal macrophages. Cells were analyzed by flow cytometry and gated on F4/80 and CD11b positive macrophages that were CFSE positive for tumor cells (Fig. S4). The antibody version of sm3E on mouse isotype IgG2a (mIgG2a) served as a positive control of phagocytosis, while dsSSMSA-L and uncoated cells ("cells only") were negative controls. Increased phagocytosis only occurred with MC38-CEA and B16-CEA. The Fn3s that bound to the activating receptors mFc γ RI, mFc γ RIII, and mFc γ RIV promoted increased phagocytosis (Fig. 6a and b). On the other hand dsSSMSA-II did not promote phagocytosis, consistent with the fact that the II Fn3 binds to the inhibitory mFc γ RIIB. The significant increases in phagocytosis further confirmed that these Fn3s are specific for their mFc γ Rs and show proper activity. Phagocytosis was further confirmed by microscopy (Fig. 6c). This demonstrated that CFSE signal was actually from engulfed tumor cells within the macrophages, in agreement with the flow cytometry data collected. Phagocytosis was driven by mFc γ RIV with both Fn3 binders (IV1 and IV2) although they engaged at different binding sites. This demonstrated that precise stereospecific engagement of Fc γ Rs were not required for activation.

Prophylactic studies of single agent treatments

Pharmacokinetics of the dsSSMSA-Fn3 constructs confirmed beta half-lives at a range from 22–28 hours (Fig. S5). Prophylactic monotherapy tests were conducted on subcutaneous tumors of B16-CEA cells in transgenic mice endogenously expressing human CEA (CEA.Tg mice). Controls used were: PBS as a vehicle control, sm3E mIgG2a as a positive control, and dsSSMSA-L as a negative control. Results showed that both PBS and dsSSMSA-L treated tumors rapidly grew out, hence lower median survival times, whereas

sm3E mIgG2a treated tumors had delayed tumor growth, until treatment termination (Fig. 7a and S6a). PBS and dsSSMSA-L survival times were not significantly different from each other. Survival curves show that sm3E mIgG2a, dsSSMSA-I, and dsSSMSA-IV1 have significantly extended survival as compared with dsSSMSA-L. Although survival of dsSSMSA-IV2 treated mice is not statistically significantly different when compared dsSSMSA-L, there is also no statistical difference between dsSSMSA-IV2 and dsSSMSA-IV1 treatment. When dsSSMSA-I survival was compared to dsSSMSA-IV1 there is a significant difference between the two. The median survival time (Fig. 7b) for dsSSMSA-I treated mice was 35 days in comparison to dsSSMSA-L treated mice of 18 days. Treatment with dsSSMSA-IV1 treatment also worked fairly well with a median survival time of 27 days. Differences in survival times with the remaining constructs dsSSMSA-II, III, and IV2 were not statistically significant in comparison to the control dsSSMSA-L. Macrophage depletion studies with anti-CSF-1R showed that macrophages play a role in dsSSMSA-IV1 tumor growth control and overall survival (Fig. 7c and S6b). Although, there is a trend, macrophages do not play a significant role in the overall survival of dsSSMSA-I tumor control. This suggests that macrophages are involved in tumor control in combination with other immune cells expressing mFc γ RI and mFc γ RIV.

Discussion

Significant effort in antibody therapeutic development has been devoted to driving greater therapeutic efficacy by engineering interactions with Fc γ Rs. Previous work aimed at understanding Fc γ R contributions utilized Fc γ R KO mice, but unfortunately KO mice have been shown to change Fc γ R expression patterns to compensate for the lack of certain Fc γ Rs [38–40]. Instead, we have studied these interactions by creating artificial Fc γ R-monospecific opsonizing agents, invoking innate immune responses that engage individual Fc γ Rs within a wild-type immune system.

In this work, we engineered individual Fn3 using yeast display of the Fn3 scaffold to bind with specificity to murine Fc γ RI, Fc γ RIIB, Fc γ RIII, and Fc γ RIV. The five Fn3 clones: I, II, III, IV1, and IV2 show specificity to their target Fc γ R based on yeast display titrations and binding studies in the dsSSMSA-Fn3 format. The yeast display titrations showed very little cross-reactivity of the Fn3 binders to other mFc γ R.

These dsSSMSA-Fn3 constructs functionally mimic an antibody except with monovalent targeting and monospecific Fc γ R binding. Antigen-binding, FcRn-mediated lifetime extension, and Fc γ R engagement were all present in these constructs, which were modular so that the scFv could be switched out to target other antigens and the Fn3s were also easily replaced with ones of varying specificity. The MSA component extended *in vivo* serum half-life. The engineered dsSSMSA-Fn3 constructs showed specificity of the scFv to the target antigen, CEA, and simultaneously bound tumor cells and Fc γ R. These dsSSMSA-Fn3 constructs also demonstrated proper activity through specific *in vitro* macrophage phagocytosis, an appropriate model as macrophages express all four mFc γ R [14].

In the aggressive B16-CEA tumor model, prophylactic dosing of the dsSSMSA-Fn3 monotherapy that targeted activating mFc γ R (I and IV) demonstrated delayed tumor growth

until end of treatment. The greatest therapeutic effect was obtained by the mFc γ RI-targeted construct, with one of the mFc γ RIV-binding constructs failing to show significant efficacy and the other delaying tumor growth to a lesser degree than the mFc γ RI-targeted construct. These results were consistent with other evidence suggesting Fc γ RI induces a particularly strong anti-tumor efficacy in the B16 melanoma mouse model [41]. The two binders IV1 and IV2 had no statistically significant differences in survival times compared to each other, which showed that the two different epitopes targeted on mFc γ RIV are irrelevant for efficacy. Interestingly, in our model, mFc γ RIII did not have a major role in tumor clearance. The mFc γ RIII Fn3 binder had a slightly lower affinity than the other Fn3 binders, which could account for the decrease in efficacy, but was still in the affinity range of the wild-type mouse IgG2a binding affinity. Most likely, combinations of mFc γ RIII engagement with other activating mFc γ Rs would help in tumor control, since our study showed that mono-specific engagement failed tumor control for this mFc γ R.

Macrophage depletion studies demonstrated the importance of macrophages in controlling tumor growth and overall survival. In dsSSMSA-IV1 therapy, it appears that macrophages play a significant role, whereas in dsSSMSA-I therapy, macrophage depletion does not demonstrate a significant difference in overall survival. This suggests that there might be other dominant immune cell types that play a role in tumor control with both mFc γ RI and mFc γ RIV. Interestingly, complete redirection of binding activity towards activating only receptors mFc γ RIII and mFc γ RIV was still inferior at tumor control compared to the IgG. This suggests that there might be other factors that play a role in effector function in addition to the A/I ratio. For example, the IgG structure may inherently confer superior properties, as it is bivalent for tumor targeting where as the Fn3 constructs are monovalent. Therefore, the IgG could potentially have increased tumor cell engagement as compared to the dsSSMSA-Fn3s, which could explain differences in efficacy. Future factorial combination therapies with the Fn3 binders may parse out the ideal combination of activating mFc γ R engagement that results in greater survival times.

By engineering binders specific to each individual mFc γ R, we have for the first time been able to test the importance of each individual mFc γ R in anti-tumor effector function from a protein engagement perspective. Engineering novel binders instead of altering the Fc portion of an antibody enabled far greater receptor specificity than previously reported. As opposed to isotype swapping, these Fn3 have greater specificity and lower cross-reactivity with other mFc γ R. These binders provide a powerful toolkit for parsing mFc γ R contributions in other models of cancer or autoimmune disease.

Materials and methods

Engineering and screening approach of Fn3s

Fn3 engineering was conducted as noted previously [31,37]. The G4 yeast surface display Fn3 library was initially screened against biotinylated mouse Fc γ Rs (detailed in supplementary materials) immobilized on biotin binder dynabeads (Invitrogen). The library was depleted of binders first to naked dynabeads and then to other irrelevant murine Fc γ Rs before enrichment of binders to the target mFc γ R. To prevent cross-reactivity of binders, two different flow cytometry sorting methods were used to isolate Fn3 binders specific to

individual mFcγR. The first method required sequential enrichments to the target mFcγR and subsequent depletions of binders to other mFcγRs. Yeast induced to express Fn3 were incubated with chicken anti-c-Myc antibody (Gallus Immunotech) to select for fully displayed Fn3s and soluble biotinylated mFcγR to select for binders. Enrichment sorting windows collected high display and high binding to target mFcγR. Depletion sorting windows collected only properly displayed Fn3s that showed no binding to the irrelevant mFcγRs. The second method consisted of two color labeling. Biotinylated mFcγRs were precomplexed in a 4:1 molar ratio to Alexa Fluorophore 488 or 647 labeled streptavidin before incubation with induced yeast. Cells that showed binding to the target mFcγR and no binding to the other mFcγRs were collected and expanded. Both methods were used to isolate Fn3 binders to individual mFcγRs. Sorting was performed on a MoFlo (Beckman Coulter) or a FACS Aria (Becton Dickinson) instrument. Sublibraries were sorted for 5 to 8 generations with mutagenesis introduced between each generation [31]. Periodic checks ensured that sublibraries maintained specificity to their target mFcγR and no cross-reactivity to other mFcγRs. From each sublibrary of binders to mFcγRI, mFcγRIIB, mFcγRIII, and mFcγRIV, 6 to 9 colonies were sequenced and unique clones were retransformed into EBY100 for display.

Epitope mapping

The ectodomain of mFcγRIV was cloned into the yeast display vector and low mutagenesis was introduced using a Mutazyme II polymerase. Based on the total residues of the mFcγRIV ectodomain, the theoretical diversity needed for a single point mutation library of the 183 residues of the ectodomain is 3.48×10^3 . The engineered mFcγRIV single point mutation library size at 4.13×10^6 sufficiently covered the diversity needed. The mFcγRIV epitope-mapping library was sorted through FACS with soluble Fn3s with c-terminal HIS6 tag, IV1 and IV2, and only properly displayed cells with no binding to the Fn3s were collected. After 3–4 enrichment sorts, individual clones were sequenced to determine mutated residues that disrupted binding.

Binding analysis

Yeast display titrations were performed as noted previously [42]. Yeast were stained for full display using a chicken anti-c-Myc antibody (Gallus Immunotech) and also incubated with different dilutions of soluble biotinylated mFcγR. Secondary labeling was performed with a goat anti-chicken Alexa Fluor 488 conjugated antibody and streptavidin conjugated with Alexa Fluor 647 at recommended dilutions. Titrations were analyzed on a FACSCalibur HTS (Becton Dickinson) instrument.

dsSSMSA-Fn3 construction

An scFv-serum albumin-Fn3 construct was engineered as a tumor targeting protein therapeutic. Different Fn3 clones were fused to the c-terminus of the MSA by a Gly₃Ser linker. The MSA and scFv were linked by a Gly₄Ser linker.

Binding Kinetics

The BLitz system (ForteBio) was used to determine binding affinities. All proteins were diluted into 1X Kinetics Buffer, 1XPBS pH 7.4 with 0.002% Tween-20 and 0.1% bovine serum albumin (BSA). Biotinylated mFc γ R was immobilized on a streptavidin biosensor at a concentration of 100nM for 180 seconds. dsSSMSA-Fn3 constructs to their respective mFc γ R were incubated with the tips at different concentrations. Association times for dsSSMSA-I, II, III, and IV2 were 240 seconds and 120 seconds for dsSSMSA-IV1. Dissociation times were 360 seconds for dsSSMSA-I, II, III, and IV2 and 180 seconds for dsSSMSA-IV1. Tips were regenerated each time for 60 seconds with 0.1M Glycine HCl pH 3.5. A new tip was used for mFc γ RIIB for each concentration since it was sensitive to Glycine regeneration.

Cell surface Fc γ R binding

The genes for full length mFc γ RI, IIB, III, and IV from cDNA prepared from the murine alveolar macrophage cell line MH-S (ATCC) were cloned into separate gWiz (Genlantis) vectors with a c-Myc tag at the N-terminus. The common gamma chain was also cloned into the gWiz vector. HEK293 cells were seeded over night at 1×10^6 cells per 10 cm dish in DMEM (Cellgro) with 10% heat inactivated FBS (Invitrogen) and 100 U/ml penicillin and 100 μ g/ml streptomycin (Cellgro). Cells were transiently transfected using transit-LT1 (Murius Bio) as per manufacturer's protocol. Transfections were with both the gWiz mFc γ R plasmid and the common gamma chain plasmid. Two days after transfection, cells were detached with Versene (Invitrogen) and resuspended in 1XPBS with 0.1% BSA (PBSA). Full expression of the mFc γ R was detected using a chicken anti-c-Myc antibody (Gallus Immunotech) and a secondary goat anti-chicken Alexa Fluor 488 (Invitrogen). Binding of the Fn3 was determined using Alexa Fluor 647 labeled dsSSMSA-Fn3. Samples were analyzed on an Accuri C6 cytometer (Becton Dickinson).

For splenocyte isolation and B-cell staining, spleens were harvested from three mice and manually dissociated between two frosted glass slides. Cells were strained through a 70 μ m strainer, pelleted, and red blood cells were lysed. Cells were resuspended in PBSA and split approximately 5×10^6 cells per sample. Samples were stained with anti-CD19 conjugated with Alexa Fluor 488 (Biolegend) and anti-CD45R/B220 conjugated with phycoerythrin (Biolegend) to detect B-Cells. Cells were then stained with Alexa Fluor 647 labeled dsSSMSA-L as a negative control and dsSSMSA-II. Samples were analyzed on an Accuri C6 cytometer (Becton Dickinson).

Phagocytosis Assay

Murine peritoneal macrophages were isolated from C57BL/6 mice four days after intraperitoneal (IP) injection of 1ml of fluid thioglycollate (Becton Dickinson, Franklin Lakes, NJ). Macrophages were seeded into a 96-well tissue culture plate at 1×10^5 cells per well and treated with 25 ng/ml of IFN- γ (Biolegend) in RPMI (Cellgro) with 10% heat-inactivated fetal bovine serum (Invitrogen) and 1X penicillin-streptomycin solution for 24–40 hours.

Cell lines (MC38, MC38-CEA, B16F10, and B16-CEA) were detached with 0.25% trypsin and 1mM EDTA, and washed and resuspended with 1XPBS and 0.1% Bovine serum albumin (PBSA) at 5×10^6 cells/ml. Cells were labeled with 5 μ M carboxyfluorescein succinimidyl ester (CFSE) for 10 minutes at room temperature in the dark. Cells were then quenched with excess PBSA and washed two more times with serum free DMEM. Cell lines were then incubated with 100nM of Sm3E mIgG2a or dsSSMSA-Fn3 for 30 minutes at room temperature in the dark. Cells incubated in protein were then transferred to the 96-well plate the peritoneal macrophages were seeded in 24–40 hours previously. Plates were incubated at 37°C with 5% CO₂ for at least 3 hours to allow for phagocytosis.

After phagocytosis, plates were pelleted, supernatants removed, and incubated with Versene (Invitrogen) for 15 min at 37°C with 5% CO₂. Cells were transferred to a new plate and washed with excess PBSA before staining for 1 hour at 4°C with anti-F4/80 Alexa Fluor 647 (Biolegend) and anti-CD11b PE (Biolegend) antibodies as macrophage markers. Plates were analyzed on a FACSCalibur HTS instrument.

Subcutaneous tumor model

Mice were maintained under specific pathogen-free conditions. All animal work was approved by the Massachusetts Institute of Technology Division of Comparative Medicine, and performed in accordance with federal, state, and local guidelines. The subcutaneous tumor model for the prophylactic monotherapy was conducted with B16-CEA cells. CEA.Tg mice [43,44] obtained from Dr. Jeffrey Scholm (National Cancer Institute) with 10 mice per group, were injected subcutaneously with 5×10^5 B16-CEA and treated with either PBS as a vehicle control, 200 μ g of sm3E mIgG2a as a positive control, or the molar equivalent of 140 μ g of dsSSMSA-Fn3. Doses were given on day 0, 2, 4, 7, 9, 11, 14, 16, and 18 after tumor inoculation. The depleting antibody anti-CSF-1R (clone AFS98) was injected i.p. at a dose of 300 μ g, starting on tumor inoculation and every other day thereafter until the last treatment. Depletion was confirmed by flow cytometry by lack of detection of CD11b and F4/80 positive cells. Mice were euthanized after tumor size reached greater than 10 mm in width and length.

Statistical Analysis

Two-way ANOVA was performed followed with the Holm-Šidák test on phagocytosis percentages (%F4/80+CD11b+CFSE+) of CEA positive and CEA negative cells. For survival times, statistical significance was determined by the Log-rank (Mantel-Cox) test. Median survival time and 95% linear confidence intervals were calculated using the survival package in R. Statistical significance was determined for p-values below 0.05.

Supplementary Material

Refer to Web version on PubMed Central for supplementary material.

Acknowledgments

This work was supported by a Sanofi-Aventis Biomedical Innovation Award and by the Koch Institute Support (core) Grant P30-CA14051 from the National Cancer Institute. We thank the Koch Institute Swanson

Biotechnology Center, Flow Cytometry Core, and Microscopy Core for their technical support. We thank Dr. Jeffrey Scholm for the gift of CEA.Tg mice and the cell lines MC38 and MC38-CEA.

Abbreviations used

mFcγR	murine Fc gamma receptor
Fn3	human tenth type III fibronectin scaffold
MSA	mouse serum albumin
CEA	carcinoembryonic antigen
scFv	single chain variable fragment
CFSE	carboxyfluorescein succinimidyl ester
dsSSMSA-Fn3	disulfide stabilized sm3E scFv Fn3 fusion
PBS	phosphate buffered saline

References

1. Adams GP, Weiner LM. Monoclonal antibody therapy of cancer. *Nat Biotechnol.* 2005; 23:1147–1157. DOI: 10.1038/nbt1137 [PubMed: 16151408]
2. Reichert JM, Valge-Archer VE. Development trends for monoclonal antibody cancer therapeutics. *Nat Rev Drug Discov.* 2007; 6:349–356. DOI: 10.1038/nrd2241 [PubMed: 17431406]
3. Harris M. Monoclonal antibodies as therapeutic agents for cancer. *Lancet Oncol.* 2004; 5:292–302. DOI: 10.1016/S1470-2045(04)01467-6 [PubMed: 15120666]
4. Boross P, Leusen JHW. Mechanisms of action of CD20 antibodies. *Am J Cancer Res.* 2012; 2:676–690. [PubMed: 23226614]
5. Nimmerjahn F, Ravetch JV. Divergent Immunoglobulin G Subclass Activity Through Selective Fc Receptor Binding. *Science.* 2005; 310:1510–1512. DOI: 10.1126/science.1118948 [PubMed: 16322460]
6. Shields RL, Lai J, Keck R, O'Connell LY, Hong K, Meng YG, Weikert SHA, Presta LG. Lack of Fucose on Human IgG1 N-Linked Oligosaccharide Improves Binding to Human FcγRIII and Antibody-dependent Cellular Toxicity. *J Biol Chem.* 2002; 277:26733–26740. DOI: 10.1074/jbc.M202069200 [PubMed: 11986321]
7. Weng WK, Levy R. Two immunoglobulin G fragment C receptor polymorphisms independently predict response to rituximab in patients with follicular lymphoma. *J Clin Oncol Off J Am Soc Clin Oncol.* 2003; 21:3940–3947. DOI: 10.1200/JCO.2003.05.013
8. Richards JO, Karki S, Lazar GA, Chen H, Dang W, Desjarlais JR. Optimization of antibody binding to FcγRIIIa enhances macrophage phagocytosis of tumor cells. *Mol Cancer Ther.* 2008; 7:2517–2527. DOI: 10.1158/1535-7163.MCT-08-0201 [PubMed: 18723496]
9. Lazar GA, Dang W, Karki S, Vafa O, Peng JS, Hyun L, Chan C, Chung HS, Eivazi A, Yoder SC, Vielmetter J, Carmichael DF, Hayes RJ, Dahiyat BI. Engineered antibody Fc variants with enhanced effector function. *Proc Natl Acad Sci U S A.* 2006; 103:4005–4010. DOI: 10.1073/pnas.0508123103 [PubMed: 16537476]
10. Tai YT, Horton HM, Kong SY, Pong E, Chen H, Cemurski S, Bennett MJ, Nguyen DHT, Karki S, Chu SY, Lazar GA, Munshi NC, Desjarlais JR, Anderson KC, Muchhal US. Potent in vitro and in vivo activity of an Fc-engineered humanized anti-HM1.24 antibody against multiple myeloma via augmented effector function. *Blood.* 2012; 119:2074–2082. DOI: 10.1182/blood-2011-06-364521 [PubMed: 22246035]
11. Jung ST, Reddy ST, Kang TH, Borrok MJ, Sandlie I, Tucker PW, Georgiou G. Aglycosylated IgG variants expressed in bacteria that selectively bind FcγRI potentiate tumor cell killing by

- monocyte-dendritic cells. *Proc Natl Acad Sci U S A*. 2010; 107:604–609. DOI: 10.1073/pnas.0908590107 [PubMed: 20080725]
12. Jung ST, Kelton W, Kang TH, Ng DTW, Andersen JT, Sandlie I, Sarkar CA, Georgiou G. Effective phagocytosis of low Her2 tumor cell lines with engineered, aglycosylated IgG displaying high Fc γ RIIa affinity and selectivity. *ACS Chem Biol*. 2013; 8:368–375. DOI: 10.1021/cb300455f [PubMed: 23030766]
 13. Sazinsky SL, Ott RG, Silver NW, Tidor B, Ravetch JV, Wittrup KD. Aglycosylated immunoglobulin G1 variants productively engage activating Fc receptors. *Proc Natl Acad Sci U S A*. 2008; 105:20167–20172. DOI: 10.1073/pnas.0809257105 [PubMed: 19074274]
 14. Nimmerjahn F, Ravetch JV. Fc γ receptors as regulators of immune responses. *Nat Rev Immunol*. 2008; 8:34–47. DOI: 10.1038/nri2206 [PubMed: 18064051]
 15. Clynes RA, Towers TL, Presta LG, Ravetch JV. Inhibitory Fc receptors modulate in vivo cytotoxicity against tumor targets. *Nat Med*. 2000; 6:443–446. DOI: 10.1038/74704 [PubMed: 10742152]
 16. Otten MA, van der Bij GJ, Verbeek SJ, Nimmerjahn F, Ravetch JV, Beelen RHJ, van de Winkel JGJ, van Egmond M. Experimental Antibody Therapy of Liver Metastases Reveals Functional Redundancy between Fc γ RI and Fc γ RIV. *J Immunol*. 2008; 181:6829–6836. [PubMed: 18981101]
 17. Bevaart L, Jansen MJH, van Vugt MJ, Verbeek JS, van de Winkel JGJ, Leusen JHW. The High-Affinity IgG Receptor, Fc γ RI, Plays a Central Role in Antibody Therapy of Experimental Melanoma. *Cancer Res*. 2006; 66:1261–1264. DOI: 10.1158/0008-5472.CAN-05-2856 [PubMed: 16452176]
 18. Peipp M, van Bueren JJJ, Schneider-Merck T, Bleeker WWK, Dechant M, Beyer T, Repp R, van Berkel PHC, Vink T, van de Winkel JGJ, Parren PWHI, Valerius T. Antibody fucosylation differentially impacts cytotoxicity mediated by NK and PMN effector cells. *Blood*. 2008; 112:2390–2399. DOI: 10.1182/blood-2008-03-144600 [PubMed: 18566325]
 19. Kaneko Y, Nimmerjahn F, Ravetch JV. Anti-Inflammatory Activity of Immunoglobulin G Resulting from Fc Sialylation. *Science*. 2006; 313:670–673. DOI: 10.1126/science.1129594 [PubMed: 16888140]
 20. Scallon BJ, Tam SH, McCarthy SG, Cai AN, Raju TS. Higher levels of sialylated Fc glycans in immunoglobulin G molecules can adversely impact functionality. *Mol Immunol*. 2007; 44:1524–1534. DOI: 10.1016/j.molimm.2006.09.005 [PubMed: 17045339]
 21. Nimmerjahn F, Ravetch JV. Antibodies, Fc receptors and cancer. *Curr Opin Immunol*. 2007; 19:239–245. DOI: 10.1016/j.coi.2007.01.005 [PubMed: 17291742]
 22. McCall AM, Adams GP, Amoroso AR, Nielsen UB, Zhang L, Horak E, Simmons H, Schier R, Marks JD, Weiner LM. Isolation and characterization of an anti-CD16 single-chain Fv fragment and construction of an anti-HER2/neu/anti-CD16 bispecific scFv that triggers CD16-dependent tumor cytotoxicity. *Mol Immunol*. 1999; 36:433–446. DOI: 10.1016/S0161-5890(99)00057-7 [PubMed: 10449096]
 23. Vallera DA, Zhang B, Gleason MK, Oh S, Weiner LM, Kaufman DS, McCullar V, Miller JS, Verneris MR. Heterodimeric Bispecific Single-Chain Variable-Fragment Antibodies Against EpCAM and CD16 Induce Effective Antibody-Dependent Cellular Cytotoxicity Against Human Carcinoma Cells. *Cancer Biother Radiopharm*. 2013; doi: 10.1089/cbr.2012.1329
 24. Behar G, Sib  ril S, Groulet A, Chames P, Pugn  re M, Boix C, Saut  s-Fridman C, Teillaud JL, Baty D. Isolation and characterization of anti-Fc γ RIII (CD16) llama single-domain antibodies that activate natural killer cells. *Protein Eng Des Sel*. 2008; 21:1–10. DOI: 10.1093/protein/gzm064 [PubMed: 18073223]
 25. Rozan C, Cornillon A, P  tiard C, Chartier M, Behar G, Boix C, Kerfelec B, Robert B, P  leg  rin A, Chames P, Teillaud JL, Baty D. Single-Domain Antibody Based and Linker-Free Bispecific Antibodies Targeting Fc γ RIII Induce Potent Antitumor Activity without Recruiting Regulatory T Cells. *Mol Cancer Ther*. 2013; 12:1481–1491. DOI: 10.1158/1535-7163.MCT-12-1012 [PubMed: 23757164]
 26. Koide A, Koide S. Monobodies: antibody mimics based on the scaffold of the fibronectin type III domain. *Methods Mol Biol Clifton NJ*. 2007; 352:95–109.

27. Koide A, Bailey CW, Huang X, Koide S. The fibronectin type III domain as a scaffold for novel binding proteins. *J Mol Biol.* 1998; 284:1141–1151. DOI: 10.1006/jmbi.1998.2238 [PubMed: 9837732]
28. Hackel BJ, Ackerman ME, Howland SW, Wittrup KD. Stability and CDR composition biases enrich binder functionality landscapes. *J Mol Biol.* 2010; 401:84–96. DOI: 10.1016/j.jmb.2010.06.004 [PubMed: 20540948]
29. Smith P, DiLillo DJ, Bournazos S, Li F, Ravetch JV. Mouse model recapitulating human Fc γ receptor structural and functional diversity. *Proc Natl Acad Sci.* 2012; 109:6181–6186. DOI: 10.1073/pnas.1203954109 [PubMed: 22474370]
30. Liu Z, Gunasekaran K, Wang W, Razinkov V, Sekirov L, Leng E, Sweet H, Foltz I, Howard M, Rousseau AM, Kozlosky C, Fanslow W, Yan W. Asymmetrical Fc engineering greatly enhances ADCC effector function and stability of the modified antibodies. *J Biol Chem.* 2013; doi: 10.1074/jbc.M113.513366
31. Chen TF, de Picciotto S, Hackel BJ, Wittrup KD. Engineering fibronectin-based binding proteins by yeast surface display. *Methods Enzymol.* 2013; 523:303–326. DOI: 10.1016/B978-0-12-394292-0.00014-X [PubMed: 23422436]
32. Graff CP, Chester K, Begent R, Wittrup KD. Directed evolution of an anti-carcinoembryonic antigen scFv with a 4-day monovalent dissociation half-time at 37°C. *Protein Eng Des Sel.* 2004; 17:293–304. DOI: 10.1093/protein/gzh038 [PubMed: 15115853]
33. Reiter Y, Brinkmann U, Lee B, Pastan I. Engineering antibody Fv fragments for cancer detection and therapy: Bisulfide-stabilized Fv fragments. *Nat Biotechnol.* 1996; 14:1239–1245. DOI: 10.1038/nbt1096-1239 [PubMed: 9631086]
34. Andersen JT, Cameron J, Plumridge A, Evans L, Sleep D, Sandlie I. Single-chain Variable Fragment Albumin Fusions Bind the Neonatal Fc Receptor (FcRn) in a Species-dependent Manner IMPLICATIONS FOR IN VIVO HALF-LIFE EVALUATION OF ALBUMIN FUSION THERAPEUTICS. *J Biol Chem.* 2013; 288:24277–24285. DOI: 10.1074/jbc.M113.463000 [PubMed: 23818524]
35. Kim J, Bronson CL, Hayton WL, Radmacher MD, Roopenian DC, Robinson JM, Anderson CL. Albumin turnover: FcRn-mediated recycling saves as much albumin from degradation as the liver produces. *Am J Physiol - Gastrointest Liver Physiol.* 2006; 290:G352–G360. DOI: 10.1152/ajpgi.00286.2005 [PubMed: 16210471]
36. Chaudhury C, Brooks CL, Carter DC, Robinson JM, Anderson CL. Albumin Binding to FcRn: Distinct from the FcRn–IgG Interaction†. *Biochemistry (Mosc).* 2006; 45:4983–4990. DOI: 10.1021/bi052628y
37. Hackel BJ, Kapila A, Wittrup KD. Picomolar affinity fibronectin domains engineered utilizing loop length diversity, recursive mutagenesis, and loop shuffling. *J Mol Biol.* 2008; 381:1238–1252. DOI: 10.1016/j.jmb.2008.06.051 [PubMed: 18602401]
38. Bruhns P. Properties of mouse and human IgG receptors and their contribution to disease models. *Blood.* 2012; 119:5640–5649. DOI: 10.1182/blood-2012-01-380121 [PubMed: 22535666]
39. Nimmerjahn F, Lux A, Albert H, Woigk M, Lehmann C, Dudziak D, Smith P, Ravetch JV. Fc γ RIV deletion reveals its central role for IgG2a and IgG2b activity in vivo. *Proc Natl Acad Sci.* 2010; 107:19396–19401. DOI: 10.1073/pnas.1014515107 [PubMed: 20974962]
40. Syed SN, Konrad S, Wiege K, Nieswandt B, Nimmerjahn F, Schmidt RE, Gessner JE. Both Fc γ RIV and Fc γ RIII are essential receptors mediating type II and type III autoimmune responses via FcR γ -LAT-dependent generation of C5a. *Eur J Immunol.* 2009; 39:3343–3356. DOI: 10.1002/eji.200939884 [PubMed: 19795417]
41. Albanesi M, Mancardi DA, Macdonald LE, Iannascoli B, Zitvogel L, Murphy AJ, Leusen JH, Bruhns P. Cutting Edge: Fc γ RIII (CD16) and Fc γ RI (CD64) Are Responsible for Anti-Glycoprotein 75 Monoclonal Antibody TA99 Therapy for Experimental Metastatic B16 Melanoma. *J Immunol.* 2012; 189:5513–5517. DOI: 10.4049/jimmunol.1201511 [PubMed: 23150715]
42. Chao G, Lau WL, Hackel BJ, Sazinsky SL, Lippow SM, Wittrup KD. Isolating and engineering human antibodies using yeast surface display. *Nat Protoc.* 2006; 1:755–768. DOI: 10.1038/nprot.2006.94 [PubMed: 17406305]

43. Clarke P, Mann J, Simpson JF, Rickard-Dickson K, Primus FJ. Mice transgenic for human carcinoembryonic antigen as a model for immunotherapy. *Cancer Res.* 1998; 58:1469–1477. [PubMed: 9537250]
44. Eades-Perner AM, van der Putten H, Hirth A, Thompson J, Neumaier M, von Kleist S, Zimmermann W. Mice transgenic for the human carcinoembryonic antigen gene maintain its spatiotemporal expression pattern. *Cancer Res.* 1994; 54:4169–4176. [PubMed: 8033149]

Highlights

- Engineered Fn3 scaffold for specific binding to each mFc γ R
- Formatted Fn3 into a tumor targeting construct as a MSA fusion, dsSSMSA-Fn3
- dsSSMSA-Fn3 constructs to activating mFc γ R drive phagocytosis
- dsSSMSA-Fn3 constructs to mFc γ RI and mFc γ RIV increases survival time of tumor bearing mice

Highlights

- Fibronectin-based scaffolds that bind with high specificity to each of the four murine Fc gamma receptors have been engineered
- Bispecific constructs targeting these binders to tumors were engineered
- Constructs targeted to activating Fc gamma receptors drive phagocytosis by macrophages in vitro
- Constructs targeting mFc γ RI and mFc γ RIV increase survival time of tumor bearing mice, to an extent similar to a murine IgG2c antibody construct

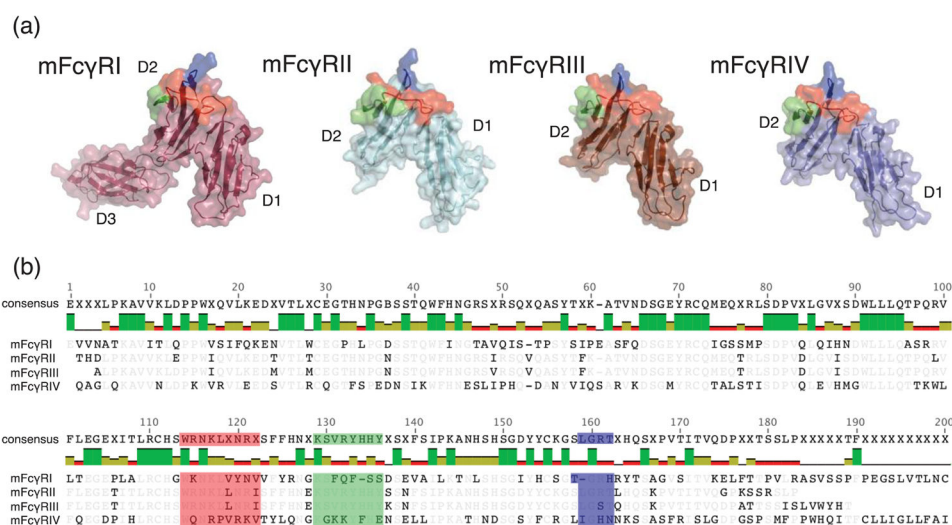


Figure 1.

Similarity between murine FcγR ectodomains. (a) Homology models of murine FcγRs (mFcγR) with their human FcγR (hFcγR) equivalent. Domains 1, 2, and 3 on the FcγRs are labeled D1, D2, and D3 respectively. Surfaces on the FcγR that interact with the BC loop (red), C'E loop (green), and FG loop (blue) of the Fc region of an IgG are highlighted. (b) Sequence alignment of domains 1 and 2 of the murine FcγRs. Only the first 200 residues of mFcγRI are shown. Surfaces on the FcγR that interact with the BC loop (shown in red), C'E loop (green), and FG loop (blue) of the Fc region of an IgG are highlighted.

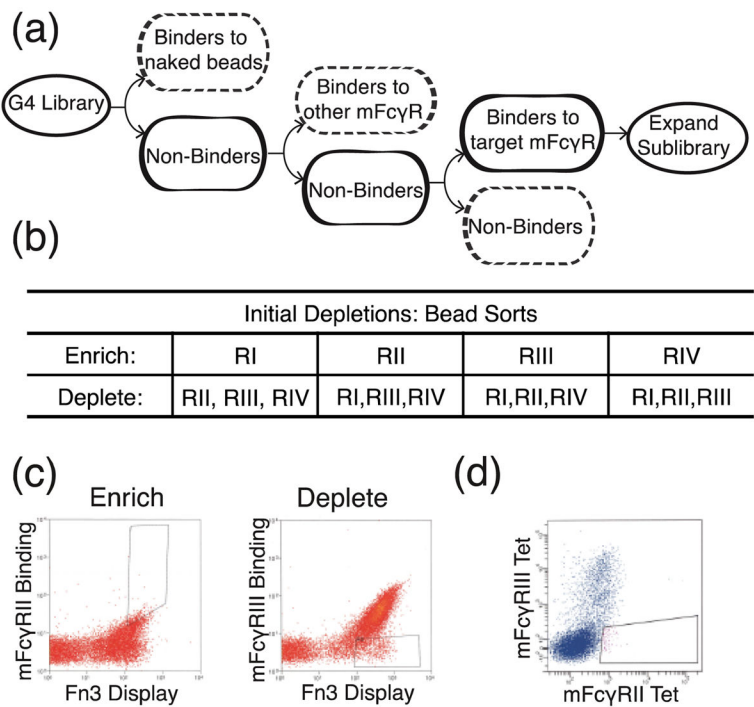


Figure 2. Sorting schematic for obtaining Fn3s with specific binding to individual FcγR. (a) Flow diagram of protocol. (b) Table of FcγR used for enrichment and depletions during initial bead sorts. (C–D) Representative flow cytometry dot plots of two different sorting protocols designed for enrichment of binders specific for individual FcγRs. (c) Enrichment of binders to the target FcγR (mFcγRII) and then depletion of cross reactive binders to another FcγR (mFcγRIII). (d) Two color sorting of FcγRs by incubating yeast with mFcγRs precomplexed with fluorophore labeled streptavidin. The collection window is drawn only on binders specific for the target FcγR (mFcγRII).

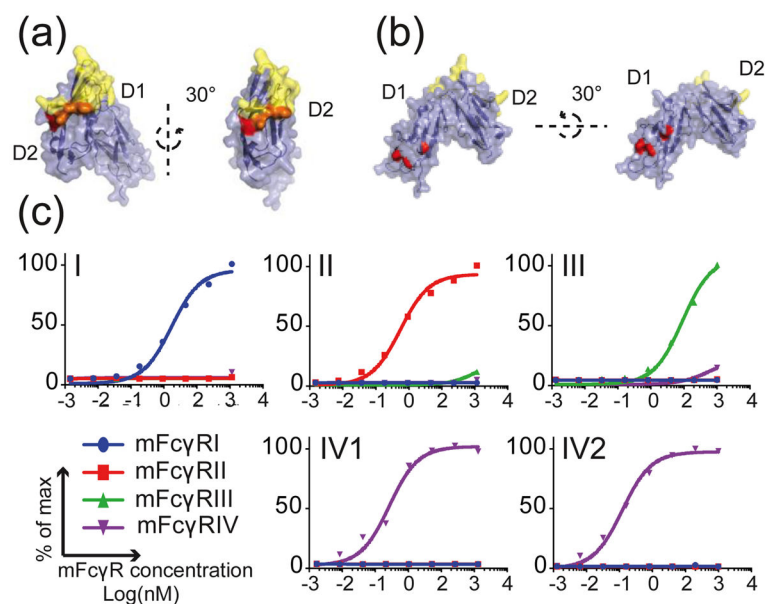


Figure 3.

Epitope map of IV binders on mFcγRIV and Fn3 binding specificity. Fn3 binding epitopes were mapped on the homology model of mFcγRIV. The IgG Fc binding region is shown in yellow. Fn3 binding epitopes are shown in red and the epitopes that overlap with the Fc binding region are shown in orange. The IV1 binding epitope is on domain 2 of the mFcγRIV shown in (a), where the right model is a 30° y-axis rotation from the left model. The IV1 binding region overlaps with that of the Fc binding epitope. The IV2 binding epitope is on domain 1 of the mFcγRIV shown in (b), where right model is a 30° x-axis rotation from the left model. The IV2 binding epitope is at a region distinct from the Fc binding epitope. (c) From top left to bottom right, yeast displaying Fn3 clones I, II, III, IV1, and IV2 incubated with titrations of all four mFcγRs. mFcγRI (blue circle), mFcγRII (red square), mFcγRIII (green triangle), mFcγRIV (purple transposed triangle). Binding detected with flow cytometry.

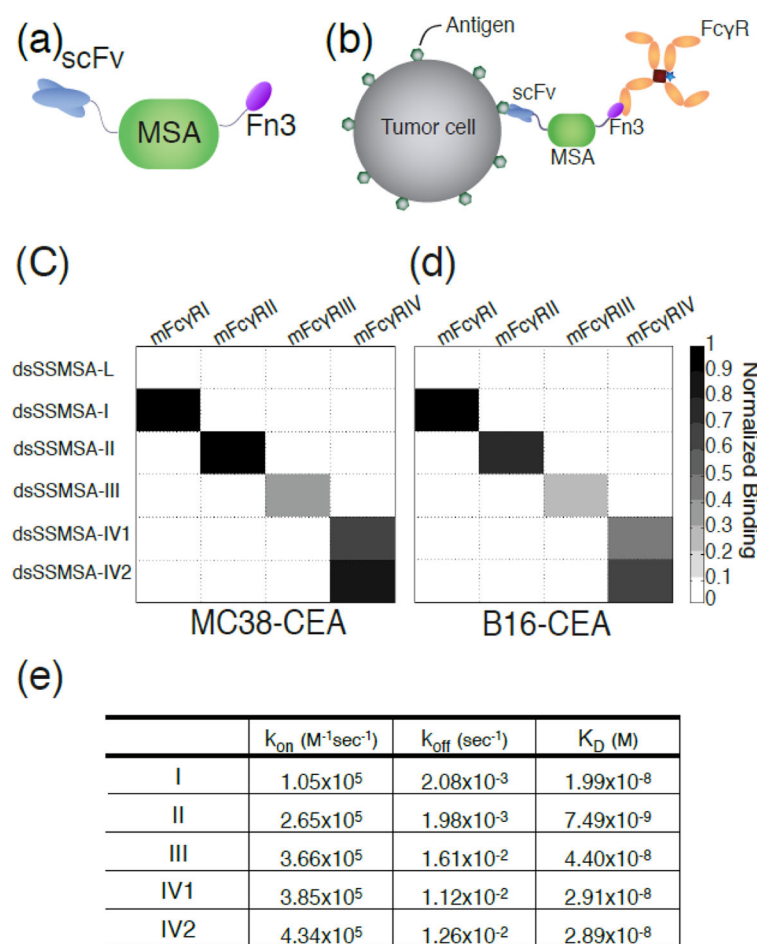


Figure 4. Characterization of Fn3s that bind individual mFcγRs. (a) Diagram of scFv-MSA-Fn3 construct. (b) Diagram of dsSSMSA-Fn3 constructs binding the tumor cell through the antigen specific scFv and engaging with tetramers of mFcγRs by the mFcγR specific Fn3. (c) Heat map showing normalized binding specificity obtained from flow cytometry of each dsSSMSA-Fn3 construct to tetramers of each mFcγR on MC38-CEA cells from the experimental set up diagramed in (b). Normalized binding gradient bar ranging from 0 to 1 depicts very strong binding as black and weak to no binding as white. (d) Same as (c) with B16-CEA cells. (e) Kinetic on rates (k_{on}), off rates (k_{off}), and affinity constants (K_D) determined by global fits to the Langmuir model (1:1 kinetics) with the BIAevaluation software.

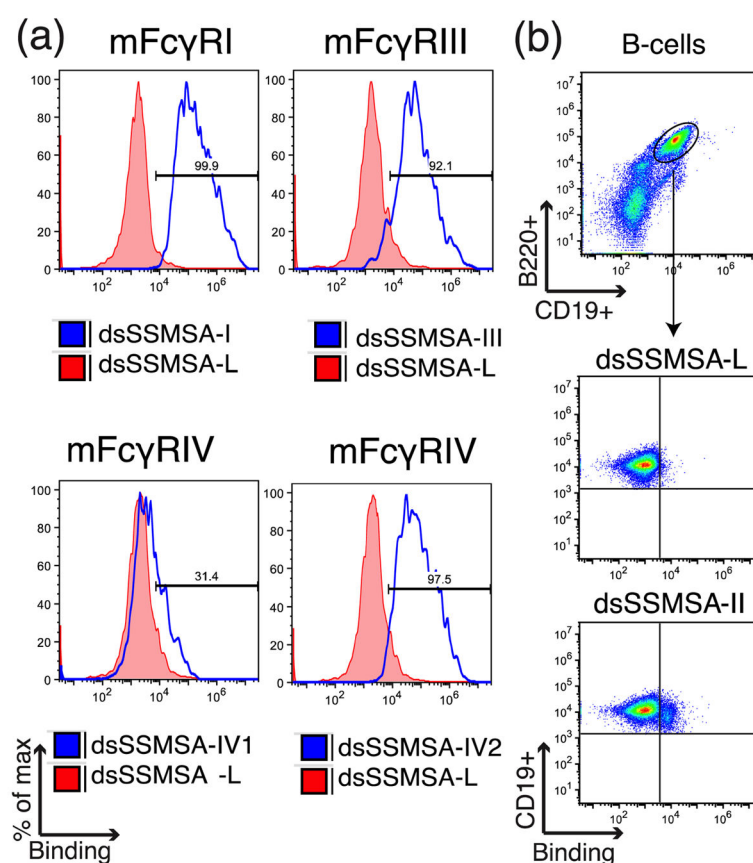
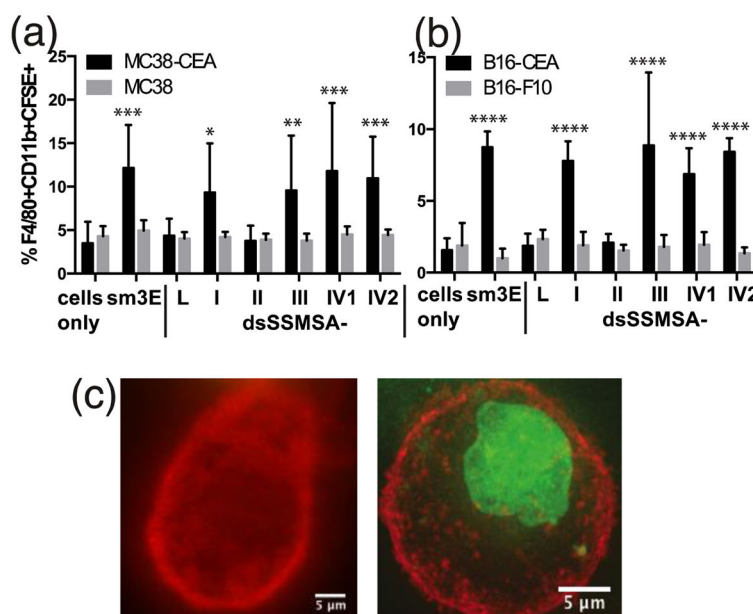


Figure 5. dsSSMSA-Fn3 constructs bind to mFcγR expressing cells. (a) Binding of dsSSMSA-Fn3 constructs with mFcγR specific Fn3 to HEK293 cells transiently transfected with activating receptors: mFcγRI, mFcγRIII, and mFcγRIV. (b) B-cells (gate shown on top) from primary mouse splenocytes labeled with the control dsSSMSA-L and dsSSMSA-II.

**Figure 6.**

Phagocytosis driven by activating mFcγRs and tumor control driven by mFcγRI. (a–b) Gray bars represent antigen negative cells (CEA-) and black bars represent antigen positive cells (CEA+). Cells were then incubated with different dsSSMSA-Fn3 constructs or sm3E IgG2a (mouse). Graphs are representative data of at least three separate experiments with four samples per condition. Data represented as mean with a 95% confidence interval. Two-way ANOVA was used to determine statistical significance between antigen positive and antigen negative cells. (a) Phagocytosis comparisons measured on MC38 and MC38-CEA cells. (b) Same as (a) with B16-F10 and B16-CEA cells. * p-val < 0.05, ** p-val < 0.01, *** p-val < 0.001, **** p-val < 0.0001 as compared to antigen negative cells (c) Microscopy of a macrophage (shown in red) on the left and a macrophage phagocytosing a tumor cell (green) on the right. Scale bar = 5 μm

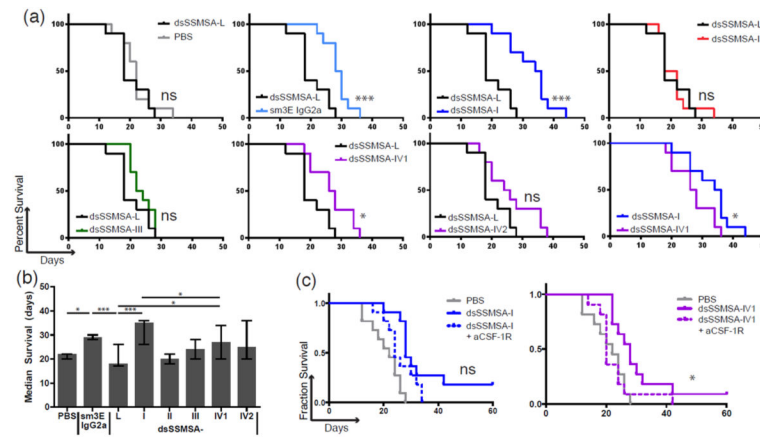


Figure 7.

Kaplan-Meier survival curves of different dsSSMSA-Fn3 treatments on mice bearing B16-CEA tumors. (a) Comparison of overall survival between treatments. Controls include PBS as vehicle, sm3E IgG2a (mouse) positive, and dsSSMSA-L negative. Plots use negative control, dsSSMSA-L, to compare mFcγR specific dsSSMSA-Fn3 treatment survival. (b) Median survival times with 95% linear confidence intervals of mice bearing B16-CEA tumors treated with the different dsSSMSA-Fn3 constructs ($n = 10$). (c) Comparison of overall survival between monotherapy treatments and monotherapy with macrophage depletion using an anti-CSF-1R antibody ($n=11$). PBS serves as the negative control. Statistical significance denoted by * for p -values < 0.05 , ** for p -values < 0.01 , *** for p -values < 0.001 , and ns for not significant.